EURASIAN JOURNAL OF MATHEMATICAL AND COMPUTER APPLICATIONS
ISSN 2306–6172
Volume 5, Issue 4 (2017) 27 – 42

INVESTIGATION OF BEHAVIOR OF THE DYNAMIC CONTACT ANGLE IN A PROBLEM OF CONVECTIVE FLOWS

Goncharova O.N., Marchuk I.V., Zakurdaeva A.V.

Abstract The two-dimensional problem of flows with a dynamic contact angle is studied in the case of an uniformly moving contact point. Mathematical modeling of the flows is carried out with the help of the Boussinesq approximation of the Navier-Stokes equations. On the thermocapillary interface the kinematic, the dynamic conditions and the heat exchange condition of third order are fulfilled. The slip conditions (conditions of proportionality of the tangential stress to the difference of the tangential velocities of liquid and wall) are prescribed on the solid boundaries kept at constant temperature. The dependence of the dynamic contact angle on the contact point velocity is investigated numerically. The presented results demonstrate the differences in the flow characteristics and contact angle behavior with respect to the different contact point velocity, friction coefficients, gravity acceleration and to amplitude of the thermal boundary regimes.

Key words: thermocapillary convection, dynamic contact angle, moving contact point.

AMS Mathematics Subject Classification: 76D05, 76D45, 76R10, 76M20.

1 Introduction

Motions of viscous incompressible fluid in domains enclosed by solid boundaries and liquid/gas interfaces are very important for theoretical study due to various applied aspects. The problems of hydrodynamics coupled with heat- and mass transfer in regions with free boundary are closely related to convective multiphase flows through porous medium, droplet evaporation and liquid films flowing over the solid heated substrate [1, 2, 3, 4, 5].

From the mathematical point of view the non-stationary fluid flows with free boundaries remain very difficult to investigate because of the dynamic contact angle problem [6, 7, 8, 9, 10, 11, 12, 13]. It occurs due to the incompatibility of the conditions on the free surface of the liquid and the conditions of adhesion on solid surface in the vicinity of moving three-phase contact line. There are various methods to tackle the problems with contact angles and to describe motion of viscous incompressible liquid in the presence of moving contact line (or contact point in the two-dimensional case). These problem statements assume the replacement of no-slip condition terms by slip conditions on some sections of the solid walls near the contact line, or the asymptotic approach, or a suggestion about equality of the contact angle to π or to "zero" etc. (see, examples in [6, 15, 16]). The solvability of the initial boundary-value problems has been proved for some mathematical models of fluid flows with dynamic contact angle

[6, 15, 16, 17]. In [15, 16, 17] it has been proved that the problem is well-posed with free boundary and dynamic contact angle on the basis of the slip conditions, when the no-slip condition on the solid boundary has been changed to the proportionality of the tangential stress to the tangential velocity. The similar conditions will be assumed to be valid in the present investigation. For the problem of fluid flow in a two-dimensional domain with free boundary and uniformly moving contact point, the existence theorem, the belonging of the velocity function to the space $H^{1,2}$ and the regularity of the free boundary have been proved in [15, 17]; the asymptotic expansions in a neighborhood of the contact points have been obtained.

The two-dimensional and axis-symmetric stationary problems have been studied in [6] in the case of small capillary numbers. The modified problem statement in [6] includes replacement of the integral equality for a generalized solution by a variational inequality; an one-sided restriction in a new problem statement consists in the sign-definiteness for the tangential component of velocity on part of the boundary.

In physical experiments [18, 19, 20, 21] it has been found that the behavior of the contact angle as a function of the contact point velocity is monotone. In the paper [22] the numerical investigations of the isothermal fluid flows with dynamic contact angle have been performed and fair agreement with the experiments has been confirmed.

One of the most important problems of the heat transfer is the extremely high evaporation rate and heat flux density at the vicinity of contact lines [23, 24, 25]. The value of the contact angle depends on the temperature of heated solid surface and on the evaporation rate as well on the velocity of the contact line. In [4] the new experimental results of changing of the contact angle during evaporation of the water drops on the open heating substrates in the case of different character of their wettability have been presented (see also [5]).

We will consider the problem of the fluid flows in a two-dimensional domain with a contact point moving with a constant velocity. The behavior of contact angle depends on the velocity of the contact point, and also on the nature of the boundary thermal conditions specified on solid walls and free thermocapillary interface. The dependence of the dynamic contact angle on the contact point velocity and the effects of the thermal regimes should be investigated.

The Navier-Stokes equations in the Oberbeck - Boussinesq approximation will be considered as a mathematical model to study two-dimensional flows of an incompressible viscous fluid with thermocapillary free boundary. The problem is studied in a quasi-stationary formulation by the introduction of coordinate system moving with the liquid. This Cartesian coordinate system is chosen so that the gravity vector is directed along the longitudinal axis (here Ox, see Fig. 1, $\mathbf{g} = (g, 0)$). Let $\mathbf{S} = (S, 0)$ be the velocity of the free boundary movement in the direction of Ox ($S = const$). We will seek such solution $(b, \mathbf{w}, \overline{p}, \Theta)$, that the following properties are satisfied: $\dfrac{d}{dt} b(t, x + St, y) - S = 0$, $\dfrac{d}{dt}\ \mathbf{w}(t, x + St, y) = 0$, $\dfrac{d}{dt}\overline{p}(t, x + St, y) = 0$, $\dfrac{d}{dt}\Theta(t, x + St, y) = 0$. Here b is the free boundary parametrization, $\mathbf{w}$ is the velocity vector of the liquid, $\overline{p}$ is the pressure, Θ is the temperature. A transition to the moving coordinate system allows one to reformulate the problem of finding the free boundary position f, velocity $\mathbf{v}$, pressure p, temperature T, which are connected with corresponding functions as follows:

$f(y) = b(t,y) - St$, $\mathbf{v}(x,y) = \mathbf{w}(t, x+St, y) - \mathbf{S}$, $p = \overline{p}(t, x+St, y)$, $T = \Theta(t, x+St, y)$ [15].

In the current paper the problem statement with dynamic contact angle is presented in the coordinate system moving with the liquid in dimensional and dimensionless forms. The dependence of the contact angle on the contact point velocity is studied numerically in the case of different values of the friction coefficients of type "liquid - solid wall". The effects of the thermal boundary regimes on the character of this dependence are investigated.

2 Statement of the problem with dynamic contact angle. Governing equations

We investigate the flows of viscous incompressible liquid in the moving coordinate system. Let $\Omega = \{(x,y) \,|\, y \in (0,l),\ f(y) < x < lx_0\}$ be the flow domain (see Fig. 1). The boundary $\partial\Omega$ of the flow region consists of three solid and one open parts: $\Gamma_0 = \{(x,y) | y \in (0,l),\ x = lx_0\}$ ("bottom"), $\Gamma_s = \{(x,y) \,|\, y \in \{0,l\},\ x \in (0, lx_0)\}$ ("lateral walls"), $\Gamma_f = \{(x,y) \,|\, y \in (0,l),\ x = f(y)\}$ (free boundary).

The system of differential equations based on the Oberbeck-Boussinesq approximation of the Navier-Stokes equations [26, 1] is used to model the flows of the liquid and to find the unknown functions, namely, the velocity vector $\mathbf{v} = (u, v)$, the temperature T, the pressure p (deviation of pressure from the hydrostatic one):

$$(\mathbf{v} \cdot \nabla)\mathbf{v} = -\frac{1}{\rho}\nabla p + \nu\Delta\mathbf{v} - \beta\mathbf{g}T, \quad div\,\mathbf{v} = 0, \tag{1}$$

$$\mathbf{v} \cdot \nabla T = \chi\Delta T. \tag{2}$$

Let $\mathbf{n}$ be the unit vector of the external normal vector; τ — the unit tangential vector to the boundary of Ω. The unknown functions $\mathbf{v}$, p, T and parametrization $f(y)$ of the free thermocapillary boundary Γ_f satisfy the boundary conditions:

$$v_n = 0 \ \text{ on } \ \partial\Omega, \tag{3}$$

$$\rho\nu\frac{\partial v_\tau}{\partial n} + \gamma v_\tau = -\gamma S \quad \text{on } \ \Gamma_s, \tag{4}$$

$$\rho\nu\frac{\partial v_\tau}{\partial n} + \gamma_0 v_\tau = 0 \quad \text{on } \ \Gamma_0, \tag{5}$$

$$\tau \cdot \mathbf{P}(\mathbf{v},p)\mathbf{n} = \nabla_\Gamma\sigma, \quad \mathbf{n} \cdot \mathbf{P}(\mathbf{v},p)\mathbf{n} = -\sigma H + \rho g f \quad \text{on } \ \Gamma_f, \tag{6}$$

$$\kappa\frac{\partial T}{\partial n} = -\delta(T - T_a), \quad \text{on } \ \Gamma_f, \tag{7}$$

$$T = T_s, \quad \text{on } \ \Gamma_s, \tag{8}$$

$$T = T_0, \quad \text{on } \ \Gamma_0, \tag{9}$$

$$f(0) = f(l) = 0. \tag{10}$$

Here $v_n = \mathbf{v} \cdot \mathbf{n}$, $v_\tau = \mathbf{v} \cdot \tau$, $\mathbf{P}(\mathbf{v},p) = -p\mathbf{I} + 2\rho\nu D(\mathbf{v})\mathbf{n}$ is the stress tensor, $D(\mathbf{v})$ is the strain rate tensor with components $D_{ij} = 0.5\big(\frac{\partial v_i}{\partial x_j} + \frac{\partial v_j}{\partial x_i}\big)$ $(i,j = 1,2;\ x_1 = x,\ x_2 = y)$,

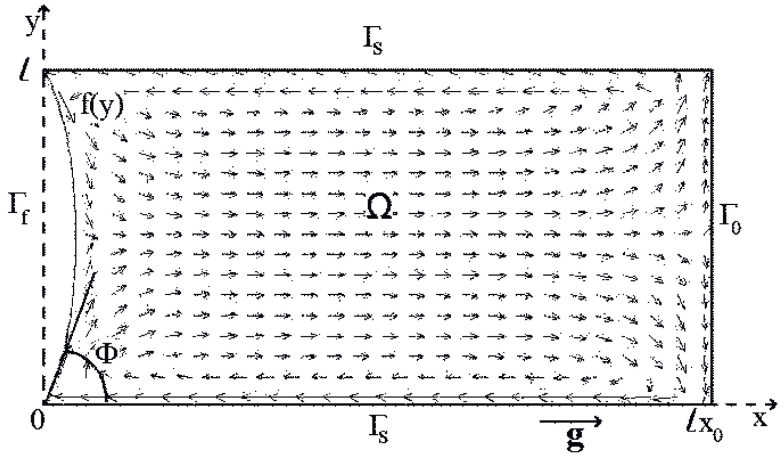

Figure 1: Geometry of flow region; topology of flow.

∇_Γ is the surface gradient (vector operator $\nabla_\Gamma = \nabla - \mathbf{n}(\mathbf{n}\cdot\nabla)$), ρ is the density, ν and χ are the coefficients of kinematic viscosity and thermal diffusivity, γ and γ_0 are the friction coefficients of type "liquid - solid wall", σ is the surface tension linearly depending on temperature ($\sigma = \sigma_0 - \sigma_T(T - T^o)$; σ_0, T^o, σ_T are the positive constants, σ_T is the temperature coefficient of surface tension), H is the free boundary curvature ($H = \Big(\dfrac{f'}{\sqrt{1+f'^2}}\Big)'$, "prime" denotes the derivative with respect to y), κ is the coefficient of thermal conductivity, δ is the interfacial heat exchange coefficient, T_a is the external temperature. The contact angle Φ at $y = 0$ is calculated as $\Phi = \arccos\Big(\dfrac{f'(0)}{\sqrt{1+f'^2(0)}}\Big)$ (see Fig. 1).

The boundary condition (3) is the non-flow condition, it includes the kinematic condition at free boundary Γ_f; (4) and (5) are the slip conditions which follow from the assumption of impulse conservation. Let us note that the condition of ideal slipping and the no-slip condition follow from (4) by $\gamma \to 0$ and by $\gamma \to \infty$, respectively. The conditions (6) are the dynamic conditions on free surface (projections of the stress vector on the tangential and normal vectors to Γ_f). The third order condition for temperature (7) or the Newton law of heat transfer is assumed to be fulfilled on the free boundary. The temperature on the lateral solid walls is kept constant (T_s and T_0, see (8), (9)). The said boundary conditions for temperature (8), (9), (7) allow one to perform the mathematical modeling of the symmetric flow picture. Thus, the results of [22] will be generalized for the case of convective fluid flow in the domain Ω with thermocapillary free boundary Γ_f.

2.1 Problem statement for the stream function and vorticity

Let the linear size l of the flow domains in the y-direction be the characteristic length. We introduce the characteristic values for the problem as follows: u_* is the characteristic velocity, $p_* = \rho u_* \nu / l$ is the characteristic pressure, T_* is the characteristic temperature

(temperature drop). The values of the scales will be specified in Section 4.

We reformulate the boundary value problem for the equations (1)-(6) in terms of new unknown functions ψ (stream functions) and ω (vorticity):

$$u = \frac{\partial \psi}{\partial y}, \;\; v = -\frac{\partial \psi}{\partial x}, \;\; \omega = \frac{\partial v}{\partial x} - \frac{\partial u}{\partial y}. \tag{11}$$

The functions ψ, ω and T will be found as the solution of the following system of equations

$$\Delta \psi = -\omega, Re\, \mathbf{v} \cdot \nabla \omega = \Delta \omega + \frac{Gr}{Re} T_y, \tag{12}$$

$$RePr\, \mathbf{v} \cdot \nabla T = \Delta T, \tag{13}$$

written in the dimensionless form. The previous notations for the input functions and variables are kept.

Direct calculations lead to the following results of writing the boundary conditions (3)-(6) in terms of ψ:

$$\psi = 0 \quad \text{on} \;\; \partial\Omega, \tag{14}$$

$$\frac{\partial^2 \psi}{\partial n^2} - H \frac{\partial \psi}{\partial n} = -Ma \frac{\partial T}{\partial \tau} \quad \text{on} \;\; \Gamma_f, \tag{15}$$

$$\frac{1}{\sqrt{1+f'^2}}(-\overline{\sigma}\sigma H' + Ma \frac{\partial T}{\partial \tau} H + \overline{g} f') = Q(\psi) \;\; \text{on} \;\; \Gamma_f, \tag{16}$$

$$\overline{\alpha}\frac{\partial^2 \psi}{\partial n^2} + \frac{\partial \psi}{\partial n} = -S \;\; \text{on} \;\; \Gamma_s \; (\text{at } y = 0), \overline{\alpha}\frac{\partial^2 \psi}{\partial n^2} + \frac{\partial \psi}{\partial n} = S \;\; \text{on} \;\; \Gamma_s \; (\text{at } y = 1), \tag{17}$$

$$\overline{\alpha}\frac{\partial^2 \psi}{\partial n^2} + \overline{\gamma}\frac{\partial \psi}{\partial n} = 0 \;\; \text{on} \;\; \Gamma_0 \; (\text{at } x = x_0). \tag{18}$$

$$\frac{\partial T}{\partial n} = -Nu(T - T_a) \;\; \text{on} \;\; \Gamma_f, \tag{19}$$

$$T = T_s \;\; \text{on} \;\; \Gamma_s \; (\text{at } y = 0 \text{ and } y = 1); \tag{20}$$

$$T = T_0 \;\; \text{on} \;\; \Gamma_0 \; (\text{at } x = x_0). \tag{21}$$

In the contact points we have

$$f(0) = f(1) = 0. \tag{22}$$

Here

$$Q(\psi) = Re\Big(\frac{\partial \psi}{\partial y}\frac{\partial}{\partial n}\frac{\partial \psi}{\partial x} - \frac{\partial \psi}{\partial x}\frac{\partial}{\partial n}\frac{\partial \psi}{\partial y}\Big) - \frac{\partial}{\partial n}\Delta\psi - 2\frac{\partial^2}{\partial \tau^2}\frac{\partial \psi}{\partial n}. \tag{23}$$

The following nondimensional parameters appear: $Re = \dfrac{v_* l}{\nu}$ is the Reynolds number, $Pr = \dfrac{\nu}{\chi}$ is the Prandtl number, $Ma = \dfrac{\sigma_T T_*}{\rho \nu v_*}$ is the Marangoni number, $Ca = \dfrac{\rho \nu v_*}{\sigma_0}$ is the capillary number, $Gr = \dfrac{\beta T_* g l^3}{\nu^2}$ is the Grashof number, $Nu = \dfrac{\delta l}{\kappa}$ is the Nusselt number.

$$\overline{\alpha} = \frac{\rho\nu}{\gamma l}, \; \overline{\gamma} = \frac{\gamma_0}{\gamma}, \; \overline{\sigma} = \frac{\sigma_0}{\rho\nu v_*} = \frac{1}{Ca}, \; \overline{g} = \frac{g l^2}{\nu v_*} = \frac{Gr}{Re(\beta T_*)}, \tag{24}$$

σ (see (16)) is the dimensionless surface tension, $\sigma = 1 - MaCa(T - T^o)$; $\dfrac{\partial}{\partial n} = \mathbf{n} \cdot \nabla$, $\dfrac{\partial}{\partial \tau} = \tau \cdot \nabla$. To reformulate the conditions (3)-(6) on free boundary and conditions (4), (5) on solid walls in terms of ψ the relations (11), $v_n = \dfrac{\partial \psi}{\partial \tau}$, $v_\tau = \dfrac{\partial \psi}{\partial n}$ and (3) are used.

To solve the problem (1)-(10) a transition to the fixed domain $\overline{\Omega} = \{[0,1] \times [0,1]\}$ is made and the following variables are introduced:

$$z = \frac{x - f(y)}{x_0 - f(y)}, \quad y = y. \tag{25}$$

Introduction of new variables (25) demands to perform the new recalculations of all the derivatives in the equations (12)-(13) and boundary conditions (11)-(23) in terms of z, y.

The equations (12) and (13) can be rewritten in new variables (25) in the following general form:

$$\frac{1}{B_{11}}\Big(\frac{\partial U}{\partial y} + \frac{\partial V}{\partial z}\Big) + G = 0. \tag{26}$$

Here

$$U = B_{11}\frac{\partial \Psi}{\partial y} + B_{12}\frac{\partial \Psi}{\partial z} + B\Psi\frac{\partial \psi}{\partial z}, \quad V = B_{12}\frac{\partial \Psi}{\partial y} + B_{22}\frac{\partial \Psi}{\partial z} - B\Psi\frac{\partial \psi}{\partial y}, \tag{27}$$

the functions Ψ, G and coefficients B_{11}, B_{12}, B_{22} and B are specified in table 1. The conditions for ψ and ω on the boundaries of $\overline{\Omega}$ are as follows:

$$\psi = 0, \ \frac{\partial \psi}{\partial y} + \overline{\alpha}\omega = -S \ \text{ on } \ y = 0, \tag{28}$$

$$\psi = 0, \ \frac{\partial \psi}{\partial y} - \overline{\alpha}\omega = -S \ \text{ on } \ y = 1, \tag{29}$$

$$\psi = 0, \ \frac{2f''}{(x_0 - f)(1 + f'^2)}\frac{\partial \psi}{\partial z} + \frac{Ma}{(x_0 - f)^2(1 + f'^2)^{5/2}}\frac{\partial T}{\partial y} - \omega = 0 \ \text{ on } \ z = 0, \tag{30}$$

$$\psi = 0, \ \frac{\overline{\gamma}}{x_0 - f}\frac{\partial \psi}{\partial z} - \overline{\alpha}\omega = 0 \ \text{ on } \ z = 1. \tag{31}$$

The thermal boundary regime for the domain $\overline{\Omega}$ defined by the conditions (7)-(9) is written now in the form:

$$T = T_s \ \text{ on } \ y = 0, \tag{32}$$

$$T = T_s \ \text{ on } \ y = 1, \tag{33}$$

$$-\frac{\sqrt{1 + f'^2}}{x_0 - f}\frac{\partial T}{\partial z} + \frac{f'}{\sqrt{1 + f'^2}}\frac{\partial T}{\partial y} = -Nu(T - T_{ex}) \ \text{ on } \ z = 0, \tag{34}$$

$$T = T_0 \ \text{ on } \ z = 1. \tag{35}$$

The equation (16) written in the variables z, y (25) will be used to compute the free boundary position (see Section 3.1).

Table 1: The coefficients in eq. (26)

Ψ	B_{11}	B_{12}	B_{22}	B	G
ω	(x_0-f)	$(z-1)f'$	$\dfrac{1+(z-1)^2f'^2}{x_0-f}$	Re	$-\dfrac{Gr}{Re}\Big(\dfrac{f'(z-1)}{x_0-f}\dfrac{\partial T}{\partial z}+\dfrac{\partial T}{\partial y}\Big)$
ψ	(x_0-f)	$(z-1)f'$	$\dfrac{1+(z-1)^2f'^2}{x_0-f}$	1	ω
T	(x_0-f)	$(z-1)f'$	$\dfrac{1+(z-1)^2f'^2}{x_0-f}$	$RePr$	0

3 Numerical investigations

The numerical algorithm of calculation of the unknown functions ω, ψ, T (see [22, 27]) is constructed with the help of the longitudinal transverse finite difference scheme known as the method of alternating directions [28, 29, 30]. To reach the stationary solution of the problem we apply a relaxation method and organize an iteration process for solving the general equation (26):

$$\Psi_t = \frac{\lambda}{B_{11}}\big(U_y + V_z\big) + \lambda G. \tag{36}$$

Here λ is an iteration parameter. To discretize in time we choose a time stepsize Δt and define $t_k = k\Delta t$ $(k = 0, 1, 2, ...)$, $\Psi^k = \Psi(t_k, \cdot)$. As a result we obtain the finite-difference scheme in the form

$$\frac{\Psi^{k+\frac{1}{2}} - \Psi^k}{0.5\Delta t} = \frac{\lambda}{B_{11}}\{U_y^k + V_z^{k+1/2}\} + \lambda G^k,$$

$$\frac{\Psi^{k+1} - \Psi^{k+\frac{1}{2}}}{0.5\Delta t} = \frac{\lambda}{B_{11}}\{U_y^{k+1} + V_z^{k+1/2}\} + \lambda G^k, \tag{37}$$

and introduce the spatial grid for its realization: (z_n, y_m); $z_n = (n-1)h_z$ $(n = 1, 2, ..., N_1)$, $h_z = 1/N$ $(N_1 = N + 1)$; $y_m = (m-1)h_y$ $(m = 1, 2, ..., M_1)$, $h_y = 1/M$ $(M_1 = M + 1)$. The derivatives in (37) will be approximated by the finite-difference analogs of second orders (see examples of approximations $V_z^{k+1/2}(x_n, y_m)$ and $U_y^k(x_n, y_m)$ in [22, 27]). The presented scheme (37) is the scheme formally of second order of approximation and unconditionally stable [28, 29, 31]. The grid function $\Psi_{n,m}$ $(\Psi(x_n, y_m) = \Psi_{n,m}\Psi^k(x_n, y_m)$ is found by solving of the systems of the linear algebraic equations

$$-a_{n,m}\Psi_{n,m-1}^{k+1/2} + b_{n,m}\Psi_{n,m}^{k+1/2} - c_{n,m}\Psi_{n,m+1}^{k+1/2} = d_{n,m},\ (n = 2, ..., N;\ m = 2, ..., M)$$

$$-a_{n,m}\Psi_{n-1,m}^{k+1} + b_{n,m}\Psi_{n,m}^{k+1} - c_{n,m}\Psi_{n+1,m}^{k+1} = d_{n,m}.\ (n = 2, ..., N;\ m = 2, ..., M) \tag{38}$$

These systems (38) are solved by the variants of the Gaussian elimination (sweep method) in the directions y and z.

3.1 Computational algorithm for f

The numerical algorithm for the problem (26)-(35) contains the important part of computation of the free boundary position. The computational algorithm for $f(y)$ (and also for $f_0(y)$) has been described in details in [22]. We limit ourselves to the following comments. We proceed from an initial situation: at given x_0 the uniformly heated to temperature T_{in} liquid is at rest (for instance, $T_{in} = T_0$, see (35)). The initial position of free boundary is defined as the solution of the problem:

$$\overline{\sigma} H_0' - \overline{g} f_0' = 0 \quad y \in (0,1), \tag{39}$$

$$\mu_0 f_0'(y) = \cos(\Phi_0) \quad \text{at} \;\; y = 0, \;\; \mu_0 f_0'(y) = -\cos(\Phi_0) \quad \text{at} \;\; y = 1, \tag{40}$$

$$f_0(0) = f_0(1) = 0. \tag{41}$$

The volume of the liquid is calculated:

$$\int_0^1 \big(x_0 - f_0(y)\big) dy = V. \tag{42}$$

Here Φ_0 is the static contact angle; its value is known [32, 20], $\mu_0 = \dfrac{1}{\sqrt{1+f_0^2}}$, see (24) for notations $\overline{\sigma}$, $\overline{g}$. Note that by given volume V the value x_0 can be determined according to (42). In the following, we will seek the solution (i.e. the position of free boundary f and the unknown functions) for certain pair (V, x_0).

Let us consider the free boundary correction w: $w = f - f_0$; its search will be performed by solution of the problem:

$$(\mu_0 w')'' - \overline{\overline{g}} w' = \overline{Q} \quad \text{on} \;\; (0,1), \tag{43}$$

$$w(0) = w(1) = 0, \tag{44}$$

$$\int_0^1 w(y) dy = 0 \tag{45}$$

for given S, ψ, ω, T and f_0. Here: $\overline{\overline{g}} = \dfrac{\overline{g}}{\overline{\sigma}}$, $\overline{Q} = -\dfrac{1}{\overline{\sigma}} \dfrac{Q}{\mu_f} - \big(f'(\mu_f - \mu_0)\big)'' + \dfrac{Ma}{\overline{\sigma}} \dfrac{1}{\mu_f} \dfrac{\partial (H\,T)}{\partial \tau}\Big|_{\Gamma_f}$, $\mu_f = \dfrac{1}{\sqrt{1+f^2}}$, Q is defined according to (16) and (23), see (24). The term $\dfrac{\partial}{\partial \tau}(H\,T)\Big|_{\Gamma_f}$ in the right-hand side of $\overline{Q}$ in the equation (43) is written in terms of new variables z, y (see (25)) and calculated at $z = 0$.

The approximate value of w is constructed on the basis of the finite-difference scheme realized on an uniform grid $y_m = (m-1)h_y$ $(m = 1, 2, ..., M_1)$, $h_y = 1/M$, $M_1 = M + 1$ [22]. In the assumption of symmetry relative to the line $y = 0.5$ the computational grid is introduced so that $y_{\overline{m}} = 0.5$ $(\overline{m} = (M/2) + 1)$. As a results of introduction of the auxiliary function $q = \mu_0 w'$ the problem (43)-(45) is solved on the interval $(0, 1)$ with respect to the symmetry properties of w and antisymmetry of q relative to $y_{\overline{m}}$.

Note that in [22] a numerical algorithm of solving f_0 is proposed (see the statement (39)-(41)) with use of a computation procedure of the correction w on condition $\overline{Q} = 0$ (see (43)-(45)). Starting with $f_0^0 = 0$ we form a sequence of iterations $\{f_0^1, f_0^2, ...\}$.

3.2 General scheme of solution of the coupled problem

With given values of the static contact angle Φ_0, position of the point x_0 (or, equivalently, with given liquid volume V), and for given contact point velocity S the numerical scheme to compute an approximate solution of the presented problem (26)-(35) is organized as follows.

1. $S = 0$. We are starting with an approximation of f_0 according to the problem statement in Section 3.1 and to the algorithm constructed in [22].

2. Let $S = S + \Delta S$ (to reach a necessary value of S we fix a sufficiently small $\Delta S > 0$ and organize "step-by-step" computations for increasing S). In each step we introduce the iteration processes to compute the unknown functions T, ω, ψ with given f. The iteration processes consist of serial calculation of $\{T^{k+1}\}$, $\{w^{k+1}\}$ and $\{\omega^{k+1}\}$ (at initial stage we have $\omega^0 = 0; \psi^0 = 0; T^0 = \min\{T_g, T_b, T_s\}$).

3. The internal iteration process for ψ^s is introduced on every step k of the external iterations of $\{\omega^{k+1}\}$.

   - Stopping conditions for f, T, ω, ψ are determined by the convergence criterion of type: $\max\limits_{n,m} |\Psi^{i+1}_{n,m} - \Psi^{i}_{n,m}| < \varepsilon_\Psi \max_{n,m} |\Psi^{i+1}_{n,m}|$, where i is the iteration number, ε_Ψ is a given accuracy.

4. Computation of f is organized according to the algorithm described in Section 3.1 and [22].

5. Transition to the step (2) is carried out until S reaches the value $S_{\max}$.

The numerical algorithm used for the problems (26)-(35) has been tested with the help of a benchmark of convection in a square cavity with a heating from one side [33, 34] and also with the help of the problem of isothermal flow with dynamic contact angle [22]. A stability of the numerical algorithm, the experimental order of convergence were investigated in [22] with a sequence of grids according to the Runge rule [1, 22].

5 Numerical results

Numerical experiments are performed for water as a working liquid. The physical and dimensionless parameters of the problem are as follows: $\rho = 1$ g/cm^3, $\nu = 0.008$ cm^2/s, $\beta = 0.15 \cdot 10^{-3}$ K^{-1}, $\sigma_T = 0.1514$ dyne/(cm K), $\sigma_0 = 72$ dyne/cm, $\gamma = \gamma_0 = \{1; 100\}$ g/(cm^2 s), $\kappa = 0.144 \cdot 10^{-2}$ kal/(cm s K), $\chi = 0.14 \cdot 10^{-2}$ cm^2/s, $\delta = \{0; 2.45 \cdot 10^{-2}; 4.9 \cdot 10^{-2}\}$ kal/(cm^2 s K, $Re = 1112$, $Pr = 7$, $Gr = \{23000; 230\}$, $Ma = 21$, $Ca = 1 \cdot 10^{-5}$, $\bar{\alpha} = 0.8 \cdot 10^{-4}$, $\bar{\gamma} = 1$, $Nu = \{0; 17; 34\}$. For the characteristic velocity we choose $v_* = \left(\sigma_0 g/\gamma\right)^{1/3}$ at $g = 981$ (cm/s^2), $\gamma = 100$ (g/(cm^2 s)). The characteristic length and temperature drop are chosen equal to $l = 1$ (cm) and $T_* = 10^0 C$. We perform the calculations with different values of the coefficients of friction of type "liquid - solid wall" γ, γ_0 [20, 22] and for two different values of static contact angle

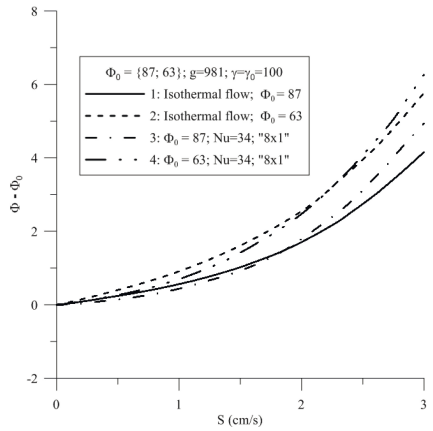

a) $\Phi_0 = 63$ and $\Phi_0 = 87$.

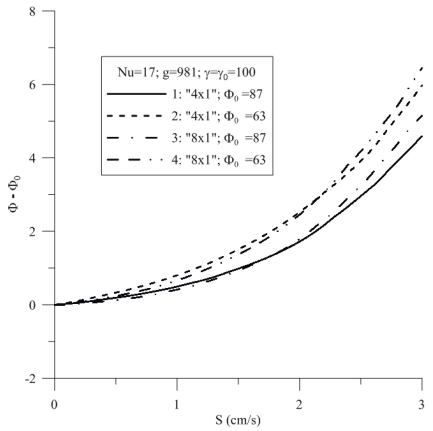

b) $\Phi_0 = 63$ and $\Phi_0 = 87$

Figure 2: Dynamic contact angle. Effects of the static contact angle. $g = 981$; $\gamma = \gamma_0 = 100$. (a) Isothermal case: $\Phi_0 = 87$ (solid line), $\Phi_0 = 63$ (dashed line); $Nu = 34$, "8×1"- regime at solid walls: $\Phi_0 = 87$ (dash-dot line), $\Phi_0 = 63$ (dash-two-dot line). (b) Regime "4×1" at solid walls: $\Phi_0 = 87$ (solid line), $\Phi_0 = 63$ (dashed line); regime "8×1" at solid walls: $\Phi_0 = 87$ (dash-dot line), $\Phi_0 = 63$ (two-dash-two-dot line).

Φ_0 ($\Phi_0 = 87^0$, $\Phi_0 = 63^0$). The calculations are carried out in the case of equal values of the coefficients γ and γ_0 ($\gamma = \gamma_0$). The thermal boundary regimes are determined by following values of the Nusselt number (see(19)) $Nu = \{0; 17; 34\}$ and for $T_a = T_0$. We also use $T_s = 8$, $T_0 = 1$ and $T_s = 4$, $T_0 = 1$ (here the dimensionless values; see (20), (21)). The thermal lateral regime is symbolically denoted as "$T_s \times T_0$" ("8×1"- regime and "4×1"- regime).

The liquid of the volume V (and the free boundary) is moving with the constant velocity in the x- direction. The contact angle (the angle between the solid wall and free boundary) is calculated in the position being inside the liquid (Fig. 1). The effects of the gravity intensity (g), friction coefficients (γ, γ_0) and of the values of the static contact angle (Φ_0) on the dependence of the contact angle Φ on the contact point velocity S are investigated. The features of this dependence relative to the thermal boundary regimes prescribed on the free and solid boundaries are investigated.

1. The influence of the friction coefficients of type "liquid - rigid wall" has been investigated. The values of the friction coefficients γ and γ_0 equal to 100 and 1 (dimensionless) have been selected. The contact angle increases more intensive for larger values of γ and γ_0 (see Fig. 3a). This trend is observed in the cases of normal and low gravity (for $g = 981$ cm/s^2 see Fig. 3a; for $g = 9.81$ cm/s^2 see Fig. 3b) for each thermal boundary regime on the rigid walls (results for the "8×1"- regime are presented in figures 2a, 3, 4b and for the "4×1"- regime — in figures 2b, 4b).

2. The features in the change of the contact angle with respect to a choice of the value of the static contact angle are demonstrated in figures 2, 3. When the static contact angle value is lesser ($\Phi_0 = 63$ in the presented investigations) the more intensive increasing of the dynamic contact angle is observed with increasing of

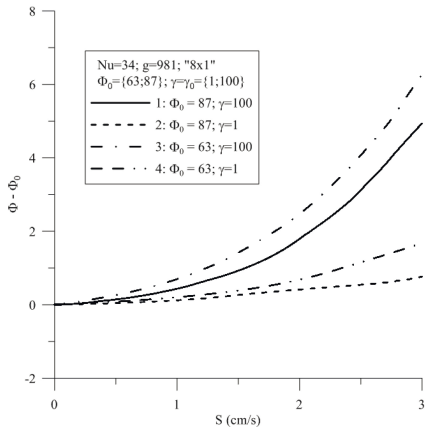

a) $\Phi_0 = 63$ and $\Phi_0 = 87$.

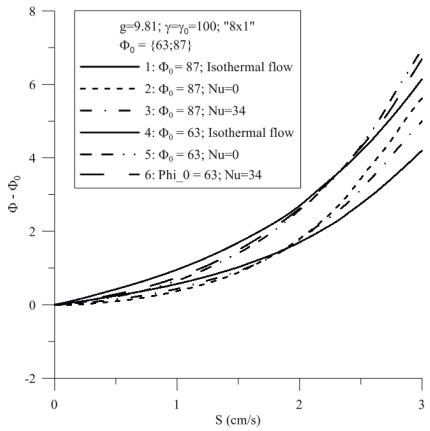

b) $\Phi_0 = 63$ and $\Phi_0 = 87$.

Figure 3: Dynamic contact angle. "8 × 1"- regime at solid walls. (a) Comparison of the effects of friction coefficients and static contact angle ($Nu = 34$, $g = 981$): $\Phi_0 = 87$ and $\gamma = \gamma_0 = 100$ (solid line), $\Phi_0 = 87$ and $\gamma = \gamma_0 = 1$ (dashed line), $\Phi_0 = 63$ and $\gamma = \gamma_0 = 100$ (dash-dot line), $\Phi_0 = 63$ and $\gamma = \gamma_0 = 1$ (two-dash-two-dot line); (b) Effects of free boundary thermal regime and static contact angle ($g = 9.81$, $\gamma = \gamma_0 = 100$). $\Phi_0 = 87$ and $\Phi_0 = 63$: isothermal case (solid lines; upper line for $\Phi_0 = 63$); $Nu = 0$: $\Phi_0 = 87$ (dashed line), $\Phi_0 = 63$ (two-dash-two-dot line); $Nu = 34$: $\Phi_0 = 87$ (dash-dot line), $\Phi_0 = 63$ (sparse dashed line).

the contact point velocity. In Fig. 3a a comparison of the results is shown for the static contact angle values equal to $\Phi_0 = 63$ and $\Phi_0 = 87$ in the case of normal gravity ($g = 981$ cm/s^2) for different values of the friction coefficients γ, γ_0 ($\gamma = \gamma_0 = 100$ or 1). In Fig. 3b we have the results in the case of low gravity ($g = 9.81$ cm/s^2) for $\gamma = \gamma_0 = 100$.

3. The influence of the thermal boundary regimes on the contact angle dynamics can be studied with the help of the figures 2b, 3b, 4a, 4b.

   - The more intensive heating of lateral walls or, equivalently, supporting of the higher temperature on the "vertical" solid walls (the "8×1"- regime), leads to the less intensity of increasing of the dynamic contact angle by comparison with the "4×1" - regime and isothermal case [22]. But such tendency is observed by beginning at the values of the contact point velocity S which are larger than $S = 2$ (see Fig. 4b; here the solid line describes the dependence of Φ on S in the isothermal case, the dashed line corresponds to the keeping at the regime "4×1"; the dash-dot line shows the dependence for the thermal regime "8×1"). The effects of larger temperature on the lateral walls are demonstrated in Fig. 2b: solid line is used for contact angle dependence at $\Phi_0 = 87$ and dashed line — at $\Phi_0 = 63$ (the dependence of Φ on S is shown for the thermal regime "4×1"). Beginning at value S approximately equal to 2, the dependence lines lie below than the corresponding lines computed for the regimes "8×1". In Fig. 2b the dashed line corresponds to the static angle equal to $\Phi_0 = 87$, and the dash-two-dot line — to the static angle

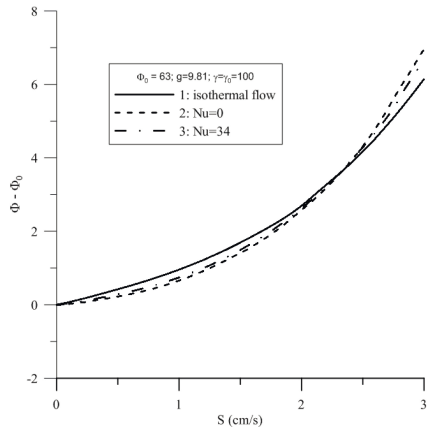

a) $\Phi_0 = 63$

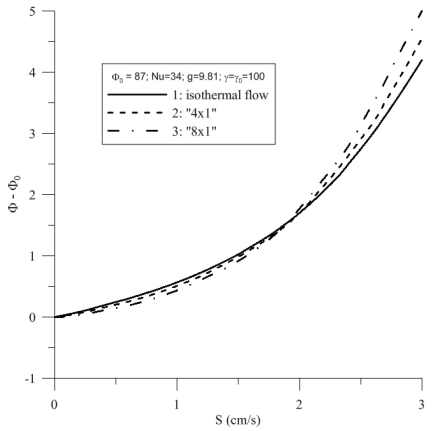

b) $\Phi_0 = 87$

Figure 4: Dynamic contact angle. Effects of thermal boundary regimes. $g = 9.81$, $\gamma = \gamma_0 = 100$. (a) "8×1"- regime at solid walls: Isothermal case (solid line), $Nu = 0$ (dashed line), $Nu = 34$ (dash-dot line); (b) $Nu = 34$: Isothermal case (solid line), "4×1" regime at solid walls (dashed line), "8×1" regime at solid walls (dash-dot line).

$\Phi_0 = 63$.

- By fixed thermal boundary regime (here the "8×1"-regime on solid walls; figures 2a, 3b, 4a) the effects of the Nusselt number on the dependency character of Φ on S is investigated. In these figures 2a, 3b, 4a a comparison with dependence of the contact angle on the contact point velocity is presented for the case of isothermal flow [22]. It is interesting to note that the graphs characterizing the behavior of the dynamic contact angle by isothermal flow are located higher than in the non-isothermal case, if the contact point velocity varies up to the value about $S = 2$ (cm/s) (changing of Φ in the case of isothermal flow is demonstrated in Fig.4a with solid line, in Fig. 2a with solid line at $\Phi_0 = 87$ and with dashed line at $\Phi_0 = 63$; in Fig. 3b the dependence of Phi on S for the isothermal case is presented with solid lines both for $\Phi_0 = 87$ and $\Phi_0 = 63$. At values of the contact point velocity larger than $S = 2$ the dynamic contact angle grows greater under action of the thermal regime. The presence of convection assists to increase the contact angle by larger value of the contact point velocity (here larger than 2 (cm/s)). In the case when $Nu = 34$ (Fig. 3b: sparse dashed and dash-dot lines; Fig. 4a: dash-dot line) the graphs of the dependence of Φ on S lie distinctly below than at $Nu = 0$. The boundary condition (19) or (34) at $Nu = 0$ determines the thermal insulation of the free boundary.

4. The numerical investigation of the contact angle dependence on the contact point velocity is carried out under conditions of normal and low gravity (for $g = 981$ (cm/s^2) see figures 2a, 2b, 3a; for $g = 9.81$ (cm/s^2) see figures 3b, 4a, 4b). The results demonstrate unequal qualitative behavior of the investigating dependence of the contact angle Φ on S and also insignificant quantitative discrepancy.

5. The topology of flow is characterized by the two-vortex flow structure that is

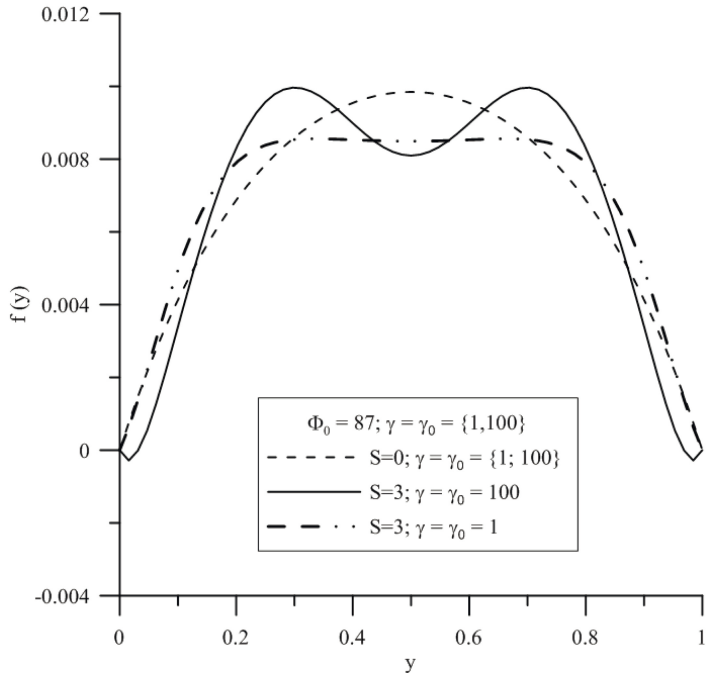

Figure 5: Free boundary. $\Phi_0 = 87$; $g = 981$; $Nu = 34$; $\gamma = \gamma_0 = \{1; 100\}$; "$8 \times 1$"-regime at solid walls. $S = 0$ and ($\gamma = \gamma_0 = 100$ or $\gamma = \gamma_0 = 1$) — dashed line, $S = 3$ and $\gamma = \gamma_0 = 100$ — solid line, $S = 3$ and $\gamma = \gamma_0 = 1$ — dash-dot line.

symmetric relative to the line $l = 1/2$ (see figures 1, 6). The rotor of velocity is especially intensive along the lateral walls $y = 0$, $y = 1$. In the case of higher value of the contact point velocity ($S = 3$ cm/s, see Fig. 6b) the two-vortex flow topology is characterized by displacement of vortex corners to the free boundary. The shapes of free thermocapillary boundary are presented in Fig. 5 for $S = 0$ (dashed line at $\gamma = \gamma_0 = 100$ and 1) and for $S = 3$ (solid line at $\gamma = \gamma_0 = 100$ and dash-dot line at $\gamma = \gamma_0 = 1$). This figure confirms the flow picture evolution by different values of the contact point velocity S.

5 Conclusions

The mathematical model and the numerical algorithm are developed to study the convective fluid flows with free boundaries and dynamic contact angle in the case, when the contact point is moving uniformly. The increasing character of this dependence on the contact point velocity has been established. The different features of dependence of the dynamic contact angle on the contact point velocity have been investigated numerically under condition of third order for thermal boundary regime at free surface and for different values of the friction coefficients of type "liquid - solid wall".

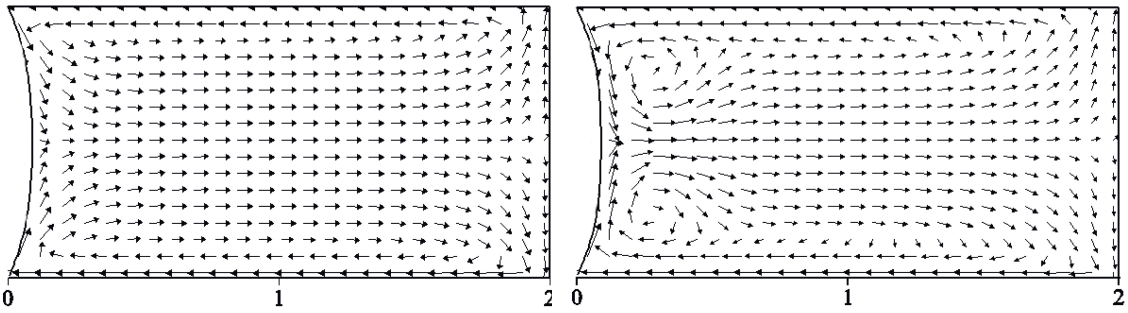

a) $S = 1$ b) $S = 3$

Figure 6: Velocity field. $S = 3$, $\Phi_0 = 63$, $g = 981$, $Nu = 17$, $\gamma = \gamma_0 = 100$, "8×1"-regime at solid walls.

Acknowledgement

This work has been supported by the Russian Science Foundation (project RSF 15-19-20049). Authors gratefully acknowledge Prof. J.-C. Legros for fruitful discussions.

References

[1] Andreev, V.K., Gaponenko, Yu.A., Goncharova, O.N., Pukhnachov, V.V., *Mathematical models of convection (de Gruyter Studies in Mathematical Physics)*, Berlin/Boston, De Gruyter, 2012.

[2] Edwards D.A., Brenner H., Wasan D.T., *Interfacial transport processes and rheology*, Boston etc., Blutterworth-Heinemann, 1991.

[3] Nepomnyashchy, A., Simanovskii, I., Legros, J.C., *Interfacial Convection in Multilayer Systems*, Springer-Verlag, New York, 2012.

[4] Gatapova E. Ya., Semenov A.A., Zaitsev D.V., Kabov O.A., *Evaporation of a sessile water drop on a heated surface with controlled wettability*, Colloids and surfaces A. Psysicochem. Eng. Aspects, Vol. 441 (2014), p. 776-785.

[5] Carle F., Semenov S., Medale M., Brutin D., *Contribution of convective transport to evaporation of sessile droplets: Empirical model*, International Journal of Thermal Sciences, Vol. 101 (2016), p. 35-47.

[6] Baiocchi C., Pukhnachov V.V., *Problems with unilateral constrains for the Navier-Stokes equations and the problem of dynamic contact angle*, J. Appl. Mech. Techn. Phys., Vol. 31, n. 2, (1990), p. 185-197.

[7] Pukhnachov V.V., Solonnikov V.A., *On the problem of dynamic contact angle*, J. Appl. Mathematics and Mechanics, Vol. 46, n. 6, (1982), p. 771-779.

[8] Schweizer B., *A well-posed model for dynamic contact angles. Preprint 98-11*, IWR, Heidelberg, 1998.

[9] Shikhmurzaev Y. D., *Mathematical modelling of wetting hydrodynamics*, Fluid Dyn. Res., n. 13 (1994), p. 45-64.

[10] Socolowsky J., *Eine verallgemeinerte Leitlinienmethode zur Berechnung mehrschichtiger Strömungen nichtlinear-viskoser Fluide*, Z. Angew. Math. Phys., n. 39 (1988), p. 221-232.

[11] Solonnikov V. A., *Solvability of a problem on the plain motion of a heavy viscous incompressible capillary liquid partially filling a container*, Math. USSR Izv., n. 14 (1980), p. 193-221.

[12] Ajaev V.S., Homsy G.M., *Modeling shapes and dynamics of confined bubbles*, Annu. Rev. Fluid Mech., n. 38 (2006), p. 277-307.

[13] Bonn D., Eggers J., Indekeu J., Meunier J., Rolley E., *Wetting and spreading*, Review of Modern Physics., Vol. 81 (2009), p. 739-805.

[14] Dussan E. B. V., Davis S. H., *On the motion of a fluid-fluid interface along a solid surface*, J. Fluid Mech. 65 (1974) 71-95.

[15] Kröner D., *Aymptotische Entwicklungen für Strömungen von Flüssigkeiten mit freiem Rand und dynamischem Kontaktwinkel. Preprint 809*, SFB72, Univ. Bonn, 1986.

[16] Kröner D., *The flow of a fluid with a free boundary and dynamic contact angle*, ZAMM. 67 (1990), p. 304-306.

[17] Kröner D., *Asymptotic expansion for a flow with a dynamic contact angle*, In the book: *Heywood J., Masuda K., Rautmann R., Solonnikov V.A. (eds.) The Navier-Stokes equations theory and numerical methods. Proc. Conf, Oberwolfach., Lect. Notes Math. 1431*, Springer Berlin, 1990, p. 49-59.

[18] Elliot G. E. P. , Riddiford A. C., *Dynamic contact angles I: The effect of impressed motion*, J. Colloid Interface Sci., Vol. 23 (1967), p. 389-398.

[19] Dussan E. B. V., *On the spreading of liquids on solid surfaces: Static and dynamic contact lines*, Ann. Rev. Fluid Mech., Vol. 11 (1979), p. 371-400.

[20] Gutoff E. B. , Kendrick C. E., *Dynamic contact angles*, AIChE J., Vol. 28 (1982), p. 459-466.

[21] Dussan E. B. V., *The moving contact line*, Waves on fluid interfaces. Proc. Univ. of Wisconsin, Madison, Univ. of Wisconsin, Madison 1982, p. 303-324.

[22] Doerfler W., Goncharova O., Kroener D., *Fluid flow with dynamic contact angle: numerical simulation*, ZAMM, Vol. 82 n. 3 (2002), p. 167-176.

[23] Marchuk I., Karchevsky A., Surtaev A., Kabov O. *Heat Flux at the Surface of Metal Foil Heater under Evaporating Sessile Droplets*, International Journal of Aerospace Engineering, art. no. 391036 (2015). (DOI: 10.1155/2015/391036)

[24] Karchevsky A.L., Marchuk I.V., Kabov O.A., *Calculation of the heat flux near the liquid-gas-solid contact line*, Applied Mathematical Modelling, Vol. 40, n. 2 (2016), p. 1029-1037. (DOI: 10.1016/j.apm.2015.06.018)

[25] Cheverda V.V., Marchuk I.V., Karchevsky A.L., Orlik E.V., Kabov O.A. *Experimental investigation of heat transfer in a rivulet on the inclined foil*, Thermophysics and Aeromechanics, Vol. 23, n. 3 (2016), p. 415-420. (DOI: 10.1134/S0869864316030112)

[26] Joseph D. D., *Stability of fluid motions*, Springer Verl., Berlin, Heidelberg, New York, 1976.

[27] Goncharova O., Zakurdaeva A., *Numerical investigation of a dependence of the dynamic contact angle on the contact point velocity in a problem of the convective fluid flow*, Journal of Siberian Federal University. Mathematics & Physics, Vol. 9, n. 3 (2016), p. 296-306.

[28] Douglas jr. J., Gunn J.E., *A general formulation of alternating direction methods; I: Parabolic and hyperbolic problems*, Numer. Math., n. 6 (1964), p. 428-453.

[29] Yanenko N.N., *The method of fractional steps: the solution of problems of mathematical physics of several variables*, Springer Verl., Berlin, Heidelberg, New York, 1971.

[30] Roache P.J., *Computational Fluid Dynamics*, Hermosa Publishers, Albuquerque, 1976.

[31] Marchuk G.I., *Splitting methods*, Nauka, Moscow, 1988 (in Russian).

[32] Landau L. D., Lifshitz E. M., *Fluid mechanics*, Pergamon Press, Oxford et al., 1959.

[33] Davis G. de Vahl, *Natural convection of air in a square cavity: a bench mark numerical solution*, Int. J. Numer. Methods Fluids, n. 3 (1983), p. 249-264.

[34] Voevodin A.F., Gocnharova O.N., *Method of computations of the two-diemnsional problems of convection on the basis of the splitting into physical processes*, Computational Technologies, Vol. 7, n. 1 (2002), p. 66-74. (In Russian).

Goncharova O.N.
Kutateladze Institute of Thermophysics SB RAS,
Russia, 630090 Novosibirsk, Ac. Lavrentieva ave., 1
and Altai State University,
Russia, 656049 Barnaul, pr. Lenina, 61
Email: gon@math.asu.ru,

Marchuk I.V.
Department of Mechanics and Mathematics,
Novosibirsk State University,
Russia, 630090 Novosibirsk, Pirogova str., 1,
Kutateladze Institute of Thermophysics SB RAS,
Russia, 630090 Novosibirsk, Lavrentieva ave, 1
and Novosibirsk State Agricultural University,
Russia, 630039 Novosibirsk, ul. Dobrolyubova, 160
Email: marchuk@itp.nsc.ru,

Zakurdaeva A.V.
Altai State University,
Russia, 656049 Barnaul, pr. Lenina, 61
Email: alla2300@bk.ru

Received 03.10.2017, Accepted 09.10.2017